Development of Multi-Stage Photocatalytic Reactors for Air Purification

D. V. KOZLOV and A. V. VORONTSOV

Boreskov Institute of Catalysis, Siberian Branch of the Russian Academy of Sciences,
Pr. Akademika Lavrentyeva 5, Novosibirsk 630090 (Russia)

E-mail: kdv@catalysis.ru

Abstract

Basic principles are considered concerning the action of photocatalysts in deep oxidation of organic compounds containing in air. Within the framework of the Langmuir-Hinshelwood model, kinetic parameters were calculated concerning the photo-oxidation process for a number of substances (the rate constant and adsorption constants) were then used for designing reactors for air purification. It is demonstrated that for increasing the rate of photocatalytic oxidation it is necessary to optimize the geometry of a photocatalytic filter, as well as to use inorganic air-penetrable materials (glass fibre cloth and foamed ceramics) as carriers for a photocatalyst. In addition, the efficiency of air purification could be enhanced through the use of multi-stage reactor wherein air under purifying passes successively the stages of electrostatic filtration, adsorption and photocatalytic treatment. An example of the proposed concept of multi-stage air purification was demonstrates at the Luch Co. (Novosibirsk).

Key words: photocatalytic oxidation, titanium dioxide, reactors for air purification, volatile organic compounds, electrostatic filtration, adsorption

INTRODUCTION

In recent decades, in connection with the rapid development of industry and transport, the humanity faced a number of challenges, primarily of environmental property. One of the most urgent problems is presented by the problem of air pollution with volatile organic compounds (VOCs). The sources of such substances could be presented by industrial emissions and transport [1], as well as materials used for interior decoration. The concentration values of these substances are often small, but a constant contact with them and inhalation of their vapours could be of health hazard for an organism [2, 3]. In this context, there is growing interest in the development of technologies for removing the VOCs in low concentration values from air.

For indoor air purification, one uses catalytic oxidation, adsorption and photocatalytic oxidation, widespread for recent decades. The catalytic oxidation of VOCs is used at the concentration values not less than 100 ppm, at high temperature (350–500 °C). At the output of the process, one could expect the formation of incomplete oxidation products of [4]. Adsorption is designed to remove pollutants from the gaseous medium via concentrating them on the surface of substances known as adsorbents (*e. g.* activated carbon or zeolites) [4]. In many cases, a contaminant is accumulated on the sorbent without changing its chemical structure. Thus, with prolonged use, the treatment efficiency is reduced, the sorbent regeneration is required, as well there is necessary to solve the problem of recycling the pollutants accumulated. In this regard, photocatalytic technology seems to be a promising method, since in most cases they provide a complete utilization of a pollutant by its deep oxidation at low concentration values.

Modern photocatalytic air purification technologies are based on using titanium dioxide as a photocatalyst, the anatase crystalline modification with a high specific surface area, for example Hombikat UV100 (Sachtleben Chemie GmbH). Under the influence of UV radiation

with the wavelength $\lambda < 400$ nm, in the bulk and on the surface of TiO_2 there are highly reactive species and structures formed, such as electron vacancies (h^+), so-called holes, and OH^- radicals with a high oxidizing reactivity. In particular, the oxidation potential of photogenerated holes with respect to the normal hydrogen electrode is equal to about $+3$ V [5] exceeding the oxidation potential of molecular fluorine ($E^0_{F_2/2F^-} = +2.87$ V) [6]. Thus, almost all the compounds adsorbed on the TiO_2 surface could be oxidized to yield inorganic substances (CO_2, H_2O, and mineral acids).

This paper summarizes the results of eight years of research work those were focused on the development of reactors for photocatalytic air purification. First, we studied photocatalytic properties of a series of titanium dioxide samples to perfect the method for the synthesis of active photocatalysts for industrial applications. Then we performed searching suitable carriers for the photocatalyst and optimizing the geometry of a photocatalytic filter. In addition, we investigated the effect of sorbents on the kinetics of photocatalytic processes. All this allowed us to construct a multi-stage photocatalytic reactor, whose production is being developed at one of the industrial enterprises of the Novosibirsk Region.

MECHANISMS OF PHOTOCATALYTIC REACTIONS

It is generally accepted that the main contribution to the mechanism of photooxidation is drawn by photogenerated holes (h^+) and OH^- radicals. One could distinguish the following basic stages concerning the formation mechanism for these highly reactive species [7−9]:

$$TiO_2 + h\nu \rightarrow h^+ + e^- \qquad (1)$$
$$H_2O(ads.) \rightarrow OH^- + H^+ \qquad (2)$$
$$OH^- + h^+ \rightarrow OH^· \qquad (3)$$
$$O_2(ads.) + e^- \rightarrow O_2^- \qquad (4)$$
$$2O_2^- + 2H_2O(ads.) \rightarrow 2OH^· + 2OH^- + O_2 \qquad (5)$$

The holes (h^+), formed in course of TiO_2 irradiation by UV light with the wavelength $\lambda < 400$ nm, can interact with adsorbed water molecules $H_2O(ads.)$ to form $OH^·$ radicals, whereas the conversion of photogenerated electrons occurs *via* the two successive stages: 1) electron transfer from the bulk or the surface of TiO_2 to the adsorbed oxygen molecule $O_2(ads.)$, step (4), 2) the interaction O_2^- with the O-adsorbed water to form $OH^·$ radicals, step (5). The charge is not accumulated on the surface of TiO_2; therefore, all these reactions occur simultaneously. Thus, one could conclude that the efficient formation of highly reactive particles (radicals, primarily $OH^·$) requires not only for irradiating the surface with UV light, but also for the presence of water vapour and oxygen.

Let us consider the mechanism of photocatalytic oxidation for one of the most common VOCs such as formaldehyde [10]. It is believed that $OH^·$ radicals and holes interact with adsorbed molecules *via* the reactions as it follows

$$HCHO(ads.) + OH^· \rightarrow HCO^· + H_2O \qquad (6)$$
$$HCO^· + OH^· \rightarrow HCOOH(ads.) \qquad (7)$$
$$HCOOH(ads.) + 2h^+ \rightarrow CO_2 + 2H^+ \qquad (8)$$
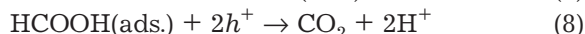
Reaction (8), to all appearance, consists of several simple reactions. In addition, it should be noted that the photooxidation of most organic compounds results in a series of successive stages of the interaction between adsorbed organic molecules with $OH^·$ radicals and the holes yielding the formation of organic acids and aldehydes those are well adsorbed on the surface of TiO_2. For example, the oxidation of ethyl alcohol vapour, alongside with CO_2 and water results also in the formation of acetaldehyde, formaldehyde, formic and acetic acids [11] revealed in the adsorbed state (Scheme 1). Acetaldehyde evolves into the gas phase only at high initial concentration values of C_2H_5OH due to the competitive adsorption (as to compare with well-adsorbed ethanol).

Thus, organic acids and aldehydes usually undergo a series of successive transformations

Ethanol

Acetaldehyde

Carbon dioxide   Acetic acid   Formaldehyde

Formic acid
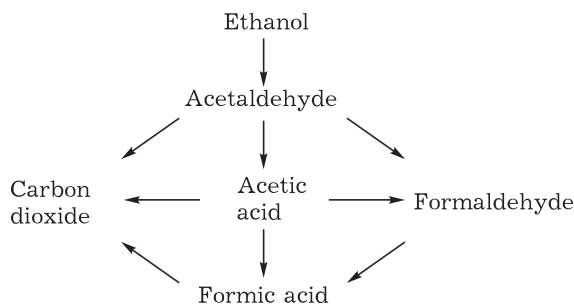
Scheme 1. Reaction of the photocatalytic oxidation of ethanol vapour on TiO_2 according to [11].

TABLE 1

Quantum efficiency of acetone vapour oxidation for different TiO_2 samples depending on the method noble metal application and on the concentration of an aqueous H_2SO_4 solution used for pretreatment

Methods of modifying	Quantum efficiency (φ), %	Ref.
Initial TiO_2 (Hombifine N)	62	[12]
(0.5 % Pt + 0.5 % Pd)/TiO_2, applied separately *via* reducing H_2PtCl_6 and $PdCl_2$ with the help of $NaBH_4$	75	[12]
(0.5 % Pt + 0.5 % Pd)/TiO_2, obtained *via* reducing double complex salt $Pd(NH_3)_4PtCl_6$ with the help of $NaBH_4$	93	[12]
TiO_2, treated with 1 M aqueous 1 M H_2SO_4	68	[22]
The same, with 4 M aqueous H_2SO_4	71	[22]
The same, with 10 M aqueous H_2SO_4	76	[22]

on the surface of TiO_2, without evolving into the gas phase; hence, no contamination of the purified air with reaction intermediates occurs in the course of the photocatalytic oxidation of organic compounds. Only the final products of oxidation such as CO_2 and H_2O are evolved into the gas phase.

KINETICS OF PHOTOCATALYTIC REACTIONS

Influence of the method of synthesizing the photocatalytically active titanium dioxide

As a raw material, we used commercial grade Hombifine N titanium dioxide (Sachtleben Chemie GmbH) representing anatase with the BET specific surface $S_{BET} = 347$ m^2/g. We used two ways to modify the initial photocatalyst: 1) the application of noble metals Pt and Pd [12], 2) sulphuric acid treatment [13]. Modified samples were tested within a flow-circulation setup [13]. The quantum efficiency of acetone vapour photocatalytic oxidation which occurs according the gross reaction

$$CH_3COCH_3 + 4O_2 \xrightarrow{h\nu,\ TiO_2} 3CO_2 + 3H_2O \qquad (9)$$
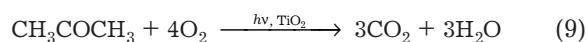
was determined by the formula [14]

$$\varphi = n[W/IS] \cdot 100\ \%$$

Here W is the rate of photooxidation of acetone, mol/s; I is the intensity of incident light mol/(cm$^2 \cdot$ s); S is the area of the illuminated sample, cm^2; n is the total change in the oxidation state of carbon atoms in the transition

from reactants to products. For the reaction (9) $n = 16$.

The processing conditions and the quantum efficiency of the catalysts synthesized are presented in Table 1. The results obtained indicate that the modification of TiO_2 surface by nanoscale metallic systems (*e. g.*, alloy Pt/Pd) results in increasing the quantum efficiency of acetone oxidation from 62 to 93 % [12]. The studies of the fundamental reasons for this effect are performed at the present time, too. However, it is believed that such an increase in the activity is directly related to the changes in the energy parameters of the individual stages of photoprocesses (changing the energy of adsorption, appearing the dark stages of reactions, *e. g.* chemisorption on metallic nanoparticles) as well as with a decrease in the recombination level of photogenerated charge carriers due to their better separation resulting from the accumulation of electrons in metallic nanoparticles [15].

The acidic treatment of TiO_2 surface also results in an increase in the quantum efficiency of the photo processes from 62 to 76 %, *i. e.* more than by 20 % (see Table 1). The causes of this phenomenon were studied in more detail. It was established that changing the adsorption energy of products and intermediates occurs at the individual stages of photoprocesses. In addition, separate dark stages are accelerated, which was demonstrated by the example the hydrolysis of a molecule of the of
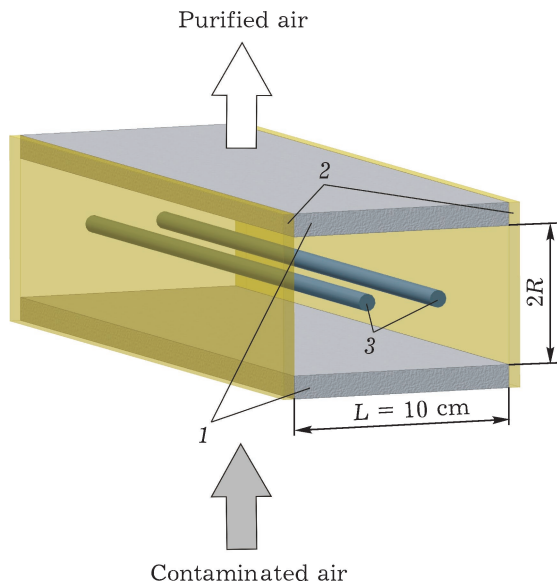
Fig. 1. Scheme of a photocatalytic unit with planar symmetry: *1* − porous carrier with photocatalyst, *2* − lateral reflectors, *3* − UV lamps.

methanephosphonic acid dimethyl ester $(CH_3O)_2P(O)CH_3$. In this case, the hydrolysis represents the first stage of the photooxidation process:

$$(CH_3O)_2P(O)CH_3 + 2H_2O \xrightarrow{TiO_2} 2CH_3OH$$
$$+ (HO)_2P(O)CH_3 \qquad (10)$$
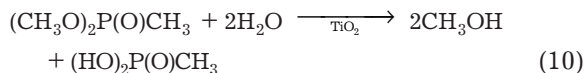
Optimizing the photocatalytic filter geometry

The next question which required for study consisted in the optimization of the geometry of the photocatalytic unit to provide the most complete use of UV lamp radiation. We have chosen a plane-parallel geometry, when the plates of a porous carrier are arranged transversely to the direction of air flow. The illumination was performed using UV lamps, as demonstrated in Fig. 1.

According to existing concepts, the rate of the most of photocatalytic reactions (W_{ox}) depends on the intensity of incident light (I) in a nonlinear manner:

$$W_{ox} = k_{eff}I^aSf(C) \qquad (11)$$

Here k_{eff} is the effective rate constant; S is the illuminated surface area; $f(C)$ is the functional dependence of the concentration values of reagents; a is a coefficient which varies within in the range of $0.5 \leq a \leq 1$ [16]. In particular, according to [16], at the intensity

of ultraviolet light flux being higher than $2 \, mW/cm^2$ the photooxidation rate for acetone was proportional $I^{0.7}$, *i. e.*, $a = 0.7$.

A possible explanation of such dependence of the reaction rate on the intensity of incident light flux consists in the fact that for a high intensity of radiation the probability of charge carrier recombination (the reaction between electrons and holes) increases [17]. Therefore, when the incident light intensity at a photocatalyst surface area is twice higher than the intensity at the adjacent area, the reactivity of the first area would only 1.6-fold as compared to the reactivity of the second one, *i. e.*, there is an increase in proportion $I^{0.7}$.

In this connection, it was necessary to calculate an optimal distance from lamps to the surface of porous media with the photocatalyst, since this parameter determines the uniformity of the surface illumination. The calculations were performed using the Monte Carlo method, where the entire surface of the lamp's bulb was divided into separate point light sources [18]. It can be seen (Fig. 2) that when the lamps are located very close to the surface and the distance between the plates becomes equal to $2R = 4$ cm (curve *1*), the surface of the carrier would be illuminated in a too non-uniform manner, with a maximum difference in light intensity (I_{max}/I_{min}) amounting to 2.8 times. With
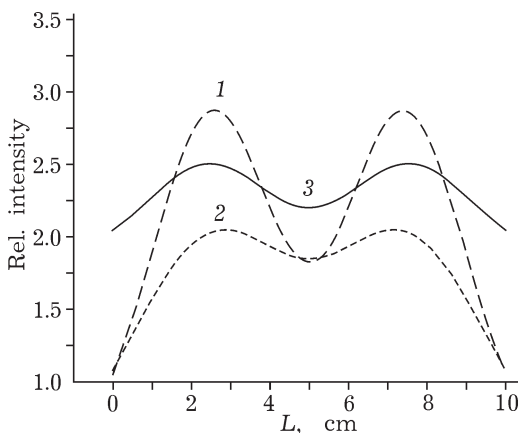
Fig. 2. Intensity light flux distribution over the surface of a flat carrier in the photocatalytic unit in the direction perpendicular to a lateral reflector, depending on the distance between the carrier plates and on the presence of the lateral of the reflector: *1* − $2R = 4$ cm, without reflectors; *2* − $2R = 6$ cm, without reflectors; *3* − $2R = 6$ cm, with reflectors.

TABLE 2

Results of integral rate calculation for photocatalytic oxidation filter, depending on the distance
between the plates of a carrier with photocatalyst and on the use of lateral reflectors

Geometry of the photocatalytic filter	$F(L)$, $L = 10$ cm	Increase compared to lowest value, %
$2R = 4$ cm, without lateral reflectors	0.120	0
$2R = 6$ cm, without lateral reflectors	0.138	+15
$2R = 6$ cm, with lateral reflectors	0.144	+20

increasing distance between the carriers up to
$2R = 6$ cm the non-uniformity of the illumina-
tion is reduced, but the difference in the illumi-
nation level is still rather great: $I_{max}/I_{min} = 2.0$.
In addition, a large part of lamp irradiation in
this situation leaks into the side openings and
does not reach the surface of the carrier. In-
deed, the area under curve *2* in 22 % less than
the area under curve *1* (see Fig. 2).

A variant with the use of lateral reflectors
was optimal one (see Fig. 2, curve *3*). The max-
imum difference between the intensities in this
case was only $I_{max}/I_{min} = 1.22$. To compare the
efficiency of air purification by photo-purifi-
ers of different geometry one could use a func-
tion of the integrated photooxidation rate, de-
pending on the local light intensity $I(l)$, absorbed
by the photocatalyst, in the form of $I(l)^a$ (for-
mula (11)):

$$F(L) = \int_0^L I(l)^a \, dl \qquad (12)$$

In equation (11), l is the coordinate, directed
along the axis L, varying within the range from
0 to 10 cm (see Fig. 1). Thus, the function $F(L)$,
where $L = 10$ cm, is proportional to the inte-
gral rate of oxidation (W_{ox}) in the case of us-
ing purification devices with a filter of a rele-
vant geometry. For the case of $a = 0.7$, using
numerical integration of the curves demonstrat-
ed in Fig. 2, we obtained integral rate values
(Table 2). It is seen that optimizing the geome-
try of a filter, the rate of the photoprocesses
could in general be increased by 20 %.

Choosing a carrier for the photocatalyst

The photocatalyst carrier should meet the
following requirements: a low aerodynamic re-
sistance (high air permeability), high mechani-
cal strength, ability to hold the particles the
photocatalyst applied, and, most important, the
carrier must be chemically resistant with re-
spect to UV light under the conditions of oxi-
dative photocatalysis. The types of carriers pre-
sented in Table 3 were used at different times
in the design of domestic reactors for photo-
catalytic air purification, and they still find an
application.

The most inexpensive carrier is presented
by polypropylene, but due to the destruction
of the polymer structure in the course of its
oxidation under the action of UV irradiation,
the material uses to lose its properties. As pro-
spective carriers, one considered foamed ceram-
ic materials made of aluminium silicates. First,
as inorganic materials, they are absolutely not
affected by photodegradation. Second, the ad-
vantages of such carriers is caused by a high
specific activity of the photocatalyst, which
could be 1.3−1.5 times greater than the specific
activity of the photocatalyst in the case when
it is applied onto a flat non-porous surface.

The effect of increasing the specific activity
per unit area of the surface of the porous
foamed ceramic carrier could be explained
within the framework of the approach
described above that is based on a power-law
dependence of the rate of photooxidation on
the irradiation intensity (eq. (11)).

The structure of a porous carrier could be
presented as a set of channels whose walls are
arranged at different angles with respect to the
direction of light flux incident along the normal
to the surface of the carrier. Let us consider
the model of a porous photocatalyst carrier,
where channels are replaced by a number of
parallel plates with the width (l) and length (h),
arranged at an angle α with respect to the
incident light with the intensity equal to I_0. The

TABLE 3

Different types of photocatalyst carriers used in modern photocatalytic air purifiers

Parameters	Porous glass	Fibrous polypropylene	Foamed ceramics	Glass fibre cloth*
Appearance	sintering at ≈400 °C			
Density, mechanical strength	Heavy, fragile	Light, flexible	Light, fragile	Light, flexible
Chemical resistance	Inert	Photodegradation under the action of UV light and TiO_2	Inert	Inert
Catalyst fixation, adhesion	Uniform, good adhesion	Non-uniform, could be blown out by air flow	Uniform, good adhesion	Uniform, good adhesion
Catalytic activity	1.0	0.8−1.0	1.4−1.5	1.2−1.3
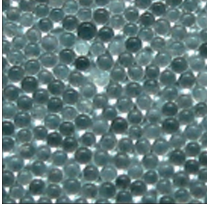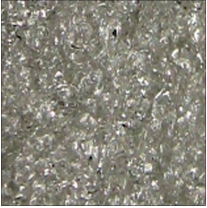
* Glass fibre cloth impregnated with aluminium salts, then dried and calcined according to the laboratory technological regulations No. 54 for the production of glass ceramic carrier IK-01-7 (Engineering specifications TU 2161-045-03533913–2007). The Al_2O_3 formed on the surface of glass fibre cloth provides its rigidity to promote a uniform application of the photocatalyst onto the surface of the carrier.

total width of the carrier is L, and the length is h (Fig. 3).

The illuminated surface area of the porous carrier, according to the model demonstrated in Fig. 3 amounts to

$$S = Lh/\cos \alpha \qquad (13)$$

The illumination intensity for the surface of inclined plates would depend on the angle α as it follows:

$$I = I_0 \cos \alpha \qquad (14)$$

Substituting (13) and (14) in eq. (11), we obtain the following expression for the rate of photooxidation depending on the angle of inclination for inclined plates:

$$W_{ox} = k_{eff} I_0^a Lhf(C)\cos^{a-1}\alpha = W_{ox,0}\cos^{a-1}\alpha \qquad (15)$$

Here $W_{ox,0}$ is the rate of photooxidation on a flat non-porous surface which is perpendicular to the direction of incident light. Thus, when the coefficient $a = 0.7$, as in [16], and the angle $\alpha = 60°$, the observed increase in rate would be: $W_{ox}/W_{ox,0} = 1/\cos^{0.3}(60°) = 1.23$ times. The use of photocatalytic filter with optimized geometry and foamed ceramic material as a carrier of the photocatalyst allowed us in general to increase the rate of air purification by about $1.2 \cdot 1.2 = 1.44$ times or by 44 %.

However, the foamed ceramics represent a delicate and expensive material, and therefore
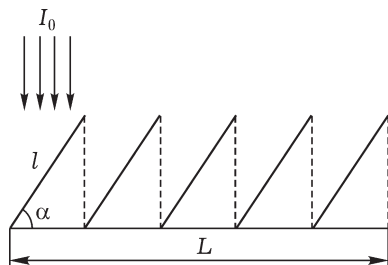
Fig. 3. Model of a porous carrier consisting of a series of parallel plates with the width l and the length h in the direction perpendicular to the Figure plane, which are arranged at the angle α with respect to the incident light with the intensity I equal to I_0. The total width of the porous carrier is L.

we suggested using wave-shaped glass fibre cloth impregnated with aluminium salts, with further calcination [19]. The wavy shape provides an effective increase in the carrier surface, reduction of its aerodynamic drag and in general provides a significant increase in the rate of air purification, only slightly being inferior to foamed ceramics in this parameter (see Table 3).

Oxidation kinetics of volatile organic compounds in a flow-through apparatus

In order to establish the rate of air purification for different types of pollutants the photocatalytic unit developed was tested under flow-through conditions in the reaction of photocatalytic vapour oxidation for a number of model air pollutants (acetone, ethanol, heptane) [20].

In the course of the experiments, the flow-through system was fed with the reaction mixture of preset composition (moisture and reagent concentration), and then, after the steady state onset, the conversion level of a reagent was determined. Most of dependence curves exhibited a characteristic appearance (Fig. 4). For example, acetone, at low concentration values was completely oxidized to yield CO_2 and H_2O in accordance with reaction (10), whereas at high (>2000 ppm) the concentration CO_2 of reaches a constant level (the maximum reaction rate was achieved) and a breakthrough of the initial reagent into the final reaction mixture was observed.

The experimental data obtained were processed using simple kinetic models such as Langmuir–Hinshelwood model:

$$A + z \underset{\longleftarrow}{\overset{K_a}{\longrightarrow}} Az \qquad (16)$$

$$Az \xrightarrow{k} P + z \qquad (17)$$

Here A is acetone; Az is acetone adsorbed on the surface; P is oxidation products (carbon dioxide and water); K_a is the constant of acetone adsorption; k is the first-order oxidation rate constant.

In particular, within the framework of this kinetic scheme, the acetone vapor concentration at the outlet of the flow system depending on the input concentration of acetone is looks like it follows:

$$A(A_0) = \left(K_a A_0 - \frac{N_0}{u} k K_a - 1 \right)$$
$$+ \sqrt{(1 - K_a A_0 + \frac{N_0}{u} k K_a)^2 + 4 K_a A_0} / 2K_a \qquad (18)$$

Here A_0 is the concentration of acetone at the inlet; A is acetone concentration at the outlet of the flow system; N_0 is the number of active sites of the photocatalyst; u is the volumetric flow rate of the reaction mixture supply. Approximation curves are presented by solid lines in Fig. 4. It was found that the rate constant k and the adsorption constant K_a are
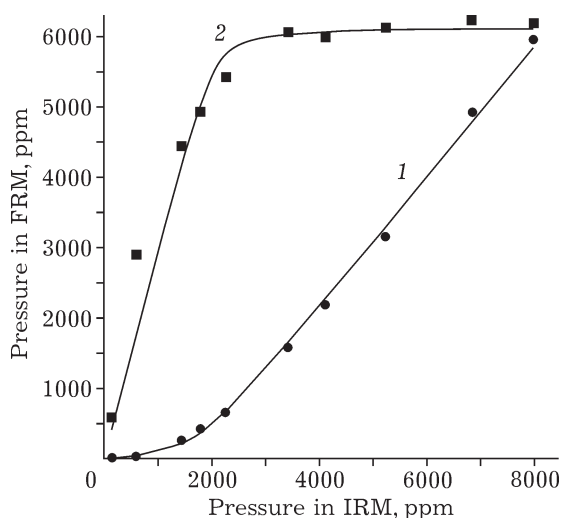
Fig. 4. Vapour pressure of acetone (1) and CO_2 (2) at the output of the photocatalytic step depending on the input vapour pressure of acetone. Solid lines demonstrate the results of approximation by the Langmuir–Hinshelwood kinetic model. IRM, FRM – initial and final reaction mixtures, respectively.

equal to $2.8 \cdot 10^{-7} \, s^{-1}$ and $0.06 \, ppm^{-1}$, respectively, which is in a good agreement with the literature data obtained using other methods.

The values calculated for adsorption constants and photooxidation rate constants for various substances used in the simulation of air purification processes in a large room. However, according to the calculations, the rate of the photooxidation process was insufficient for the rapid purification of the room wherein, for example, any bursting emissions of pollutants occur. In this context, an idea was put forward of using an adsorbent that would be placed in the purification apparatus in front of the photocatalytic unit and to quickly absorb a part of the organic pollutant, with further slowly releasing the latter in order to decompose it in the photocatalytic filter.

Effect of adsorbent on the photocatalytic oxidation kinetics for volatile organic compounds

By the example of the photocatalytic oxidation of acetone vapour in a sealed chamber we demonstrated that in the presence of an adsorbent, indeed, a more rapid removal of acetone vapour from the air quite really occurs as to compare with the case when in the reaction system there is only a photocatalyst present. From the data presented in Fig. 5, one could see that at the initial moment of time, the system with a sorbent exhibit the concentration of acetone vapour being 35−40 % lower. The time reaching the concentration of acetone amounting to 85 ppm* for the system with a sorbent is equal to 5 min, whereas that without the sorbent amounts to 55 min.

The evolution rate for the final photooxidation product such as CO_2 in the presence of the sorbent in the system exhibits a decrease, too, whereas the time required in order to reach a 100 % conversion level with respect to CO_2 increases from 150 min (with no sorbent) to 250 min (with the sorbent).

In general, as the result of computer simulation and experiments in the chamber simulating a closed room, we revealed the follow-

---

*85 ppm for acetone corresponds to $200 \, mg/m^3$ or to 1 MPC unit for working area, according to the State Standard GOST 12.1.005−88.
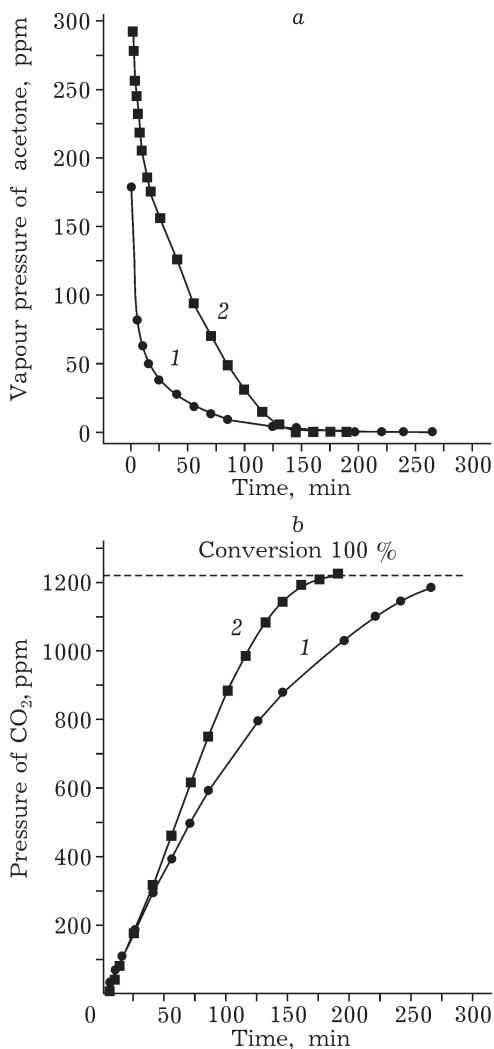
Fig. 5. Kinetics of photocatalytic oxidation for acetone vapour: a − kinetic curves of concentration decay for acetone vapour in a chamber volume (404 L in volume), b − kinetic curves for CO2 accumulation; $1, 2$ − in the presence of activated carbon and without it, respectively.

ing advantages of using an adsorption step, combined with a photo-catalytic module [21]:

1. In a closed system, the concentration of initial reagent decreases in the presence of an adsorbent under the same initial conditions.

2. Under flow-through conditions, with a bursting contaminant release, the presence of an adsorbent allows reducing the concentration of substrate at the outlet of the system, $i. \, e.$ to reduce the breakthrough in the case when the input substrate concentration is too high for being completely oxidized in a single pass.

3. When the photocatalytic reaction proceeds with the formation of intermediates, the use

of sorbent allows either reducing the concentration of an intermediate vapour (in the case of volatile intermediate) or reducing the deactivation of photocatalyst due to the intermediate transfer from the surface of photocatalyst onto the surface of the sorbent (if the intermediate is non-volatile).

MODULAR PRINCIPLE FOR ARRANGING A PHOTOCATALYTIC AIR PURIFIER

In the modern sense, the air purification involves, alongside with removing the vapours of organic contaminants, the removal of aerosols, thus modern air purifiers should be equipped with dust collectors. In our opinion, a photocatalytic air purifier should be constructed in a modular fashion, i. e., should be composed of dust, adsorption and photocatalytic filters arranged in series. The dust filter should catch spray ranging in size from 0.2 to 10 μm with the efficiency not worse than 95 % in one pass. The adsorption filter reduces catalyst de-

activation, as well as serves as a buffer in the case of high concentration values for pollutant emissions. The photocatalytic filter is basic; it provides the photocatalytic degradation of organic contaminants to yield CO_2 and H_2O. It should be noted that the adsorption filter in such a system becomes "self-regenerating" one since excess organic compounds therein could be reversibly desorbed to be oxidized on the photocatalytic filter when contacting the latter.

An example of such a construction is demonstrated in Fig. 6. As a dust filter, there is an electrostatic filter used, whose recovery consists in withdrawal from the casing, rinsing with water and drying. The adsorption filter also does not require for replacement because of the previously mentioned reasons. Thus, the photocatalytic air purifier designed is entirely composed of parts those do not require for replacement during the entire lifetime of the apparatus.

CONCLUSION

1. The photocatalytic oxidation of organic vapours using titanium dioxide allows one to perform a complete mineralization of pollutants up to CO_2 and H_2O. The application of noble metals and acidic treatment of titanium dioxide are able of increasing its photocatalytic activity to a considerable extent.

2. Studies were performed concerning the kinetics of organic vapour photo-oxidation processes. Within the framework of the Langmuir–Hinshelwood kinetic model, the values of rate constants and the adsorption constants were obtained for a number of organic compounds.

3. Choosing a carrier for the photocatalyst and optimizing the geometry of a photocatalytic filter allowed us to increase the rate of air purification by 40–50 %.

4. It was demonstrated that the use of adsorption together with the photocatalytic oxidation enhances the efficiency of air purification, resulting in a more rapid removal of substrate vapour, decreasing both intermediate concentration and catalyst deactivation.

5. The modular design of reactors for air purification allows one to perform complex air purification from aerosols and from the vapours of organic pollutants. In this case, there is no neces-
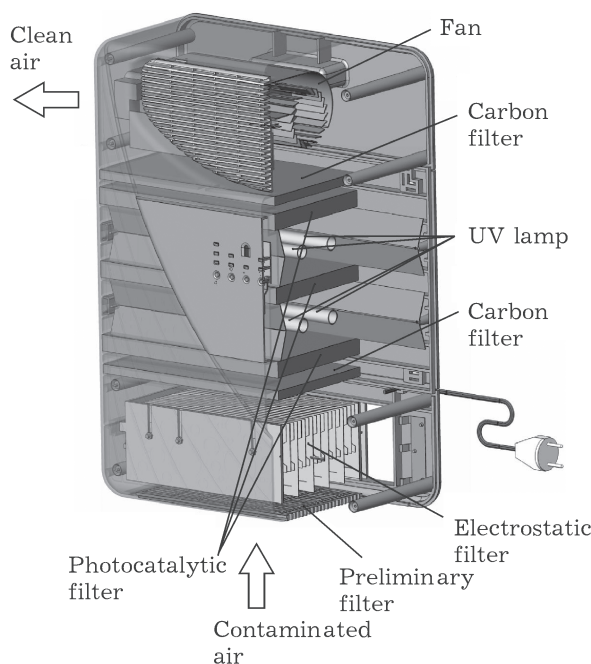
Fig. 6. Photocatalytic air purifier Luch-60 (Luch Co., Novosibirsk). Power consumption 100 W; air filtration rate up to 130 m³/h; the filtration coefficient for one passage: dust – 90 %, molecular impurities – 35 %; estimated room volume being of about 200 m³.

sary for the replacement of individual modules during all the lifetime of the air purifier.

REFERENCES

1 Riediker M., Williams R., Devlin R., Griggs T., Bromberg P., *Environ. Sci. Technol.*, 37, 10 (2003) 2084.

2 Sundeep Salvi, *Paediatric Respiratory Reviews*, 8, 4 (2007) 275.

3 Boeglin M. L., Wessels D., Henshel D., *Environ. Res.*, 100, 2 (2006) 242.

4 Faisal I. Khan, Aloke Kr. Ghoshal, *J. Loss Prevention in the Process Industries*, 13 (2000) 527.

5 Serpone N., *Solar Energy Materials and Solar Cells*, 39, 1−4 (1995) 369.

6 Rabinovich V. A., Khavin Z. Ya., Kratkiy Khimicheskiy Spravochnik, Khimiya, St. Petersburg, 1994, p. 367.

7 Ikeda K., Sakai H., Baba R., Hashimoto K., Fujishima A., *J. Phys. Chem. B*, 101 (1997) 2617.

8 Gao R., Stark J., Bahnemann D.W., Rabani J., *J. Photochem. Photobiol. A*, 148 (2002) 387.

9 Lee M. C., Choi W., *J. Phys. Chem. B*, 106 (2002) 11818.

10 Ao C. H., Lee S. C., Yu J. Z., Xu J. H., *Appl. Catal. B*, 54 (2004) 41.

11 Nimlos M. R., Wolfrum E. J., Brewer M. L., Fennell J. A., Bintner G., *Environ. Sci. Technol.*, 30 (1996) 3102.

12 RU Pat. No. 2294240, 2007.

13 Kozlov D. V., Panchenko A. A., Bavykin D. V., Savinov E. N., Smirniotis P. G., *Rus. Chem. Bull.*, 52 (2003) 1100.

14 Sha Jin, Fumihide Shiraishi, *Chem. Eng. J.*, 97 (2004) 203.

15 Peral J., Ollis D. F., *J. Catal.*, 136 (1992) 554.

16 Kim S. B., Hong S. Ch., *Appl. Catal. B*, 35 (2002) 305.

17 Vorontsov A. V., Kozlov D. V., Smirniotis P. G., Parmon V. N., *Kinet. Catal.*, 46, 3 (2005) 422.

18 Alexiadis A., *Chem. Eng. Sci.*, 61 (2006) 516.

19 RU Pat. No. 2298435, 2007.

20 Baturov I. A., Vorontsov A. V., Kozlov D. V., *Rus. Chem. Bull.*, 54, 8 (2005) 1866.

21 Selishchev D. S., Kolinko P. A., Kozlov D. V., *Appl. Catal. A*, 377 (2010) 140.

22 Kozlov D., Bavykin D., Savinov E., *Catal. Lett.*, 86, 4 (2003) 169.